

Damping properties of existing single-span prestressed concrete girder bridges with different service periods

**T. Tanaka¹, S. e Rehmat¹ and Y. Matsumoto^{1*}
and Abeykoon J. Dammika²**

¹Saitama University, Saitama, Japan

²University of Peradeniya, Peradeniya, Sri Lanka

*E-Mail: ymatsu@mail.saitama-u.ac.jp, TP: +81-(0)48-858-3557

Abstract: Invisible damages in bridges, such as corrosion of rebar, may not be detected by periodic visual inspection that is the principal method in bridge maintenance. A possible non-destructive technique which has been investigated to assist visual inspection is vibration-based structural health monitoring. The modal properties of bridges, such as the natural frequencies, mode shapes and modal damping ratios, are expected to change due to damages and/or deteriorations. In the present study, damping properties of existing PC girder bridges were identified so as to investigate the possibility of the modal damping ratios as an indicator of damage detection. Vibration measurements were made at ten single-span PC bridges with similar dimensions under normal service conditions by using wireless and wired sensor systems. Eigensystem realization algorithm (ERA) with an improved screening process was applied to extracted free vibration records. Modal properties up to the fourth vibration modes were identified for many bridges. For the third vibration mode that was identified stably in most bridges, there was a trend that the modal damping ratio of old bridges was greater than other newer bridges. Although this result does not necessarily indicate the relationship between the damage and damping property, it may support the possibility of damping in the evaluation of structural state.

Keywords: Damping properties, Eigensystem realization algorithm, Single-span prestressed concrete girder bridge

1. Introduction

There are a lot of bridges in transportation network. These bridges were constructed with about 50 years of design life. There are bridges which have been in service for over 50 years without major accidents by performing appropriate maintenance works. In Japan, more than 40% of the bridges are expected to exceed 50 years in service in 10 years' time [1]. Aging of the bridges have become a problem and appropriate maintenance is needed. Current major inspection is performed by visual inspection. However the visual inspection has some problems. For example, it is impossible to see inside of the concrete; it is difficult to inspect structural parts where sufficient space is not available for an inspector for access [2]. The structural health monitoring based on dynamic characteristics of bridges has been studied as a technique to assist the visual inspection [3]. While it has been reported that the change in damping parameters by damage and deterioration can be relatively large, compared to that in natural frequencies, the identification accuracy of damping

from measured vibration data is not high [4]. If factors affecting damping are of wide variety, physical interpretation of damping change is difficult. In addition, understanding of damping of real bridge is not sufficient.

The objectives of this study were to identify damping ratio of existing bridges with high accuracy and to elucidate their damping characteristics. In the present study, damping properties of existing PC girder bridges were identified so as to investigate the possibility of the modal damping ratios as an indicator of damage detection.

2. Target bridges

Ten existing single-span prestressed concrete girder bridges were selected for the present study. In Table 1, a list of selected bridges is shown. Those bridges were selected because they had single-span, different ages of service, and bridge length in a limited range and there was not excessive traffic volume. The ranges of completion year was 1975 to 1994. The bridge length varied

Table 1: Target bridges

Bridge No.	Completion year	Structure format	Length	Width
I (old)	1975	Pretension T beam	16.33	9.50
II (old)	1975	Pretension hollow slab	16.13	9.50
III	1976	Pretension T beam	16.60	18.00
IV	1978	Pretension T beam	19.66	13.95
V	1980	Pretension T beam	20.80	16.80
VI	1985	Pretension T beam	19.30	7.50
I (new)	1991	Pretension T beam	16.33	9.50
II (new)	1991	Pretension hollow slab	16.14	9.50
VII	1991	Pretension T beam	17.36	12.00
VIII	1994	Pretension T beam	15.00	10.00

between 15 m and 20.8 m. The structural format was either pretension T beam or pretension hollow slab. In Bridges I and II, old and new bridges are built alongside each other. The selected bridges have not been reported as damaged or deteriorated by previous visual inspection.

3. Experimental modal analysis

3.1 Vibration measurement

Vibrations of the bridges induced by ordinary road traffic were measured. Vertical acceleration was measured at several locations at each bridge by using a wired or wireless measurement system. If wiring was difficult, the wireless measurement system was used. Sampling rate of the wired measurement system was 250 samples per second, while the sampling rate of wireless measurement system was 100 samples per second.

Vibration sensors were placed at different positions to identify mode shapes of the bridges by experimental modal analysis. In Figure 1, an example of sensor position is shown. Additionally, video recording was taken so as to understand the traffic situation during the vibration measurement

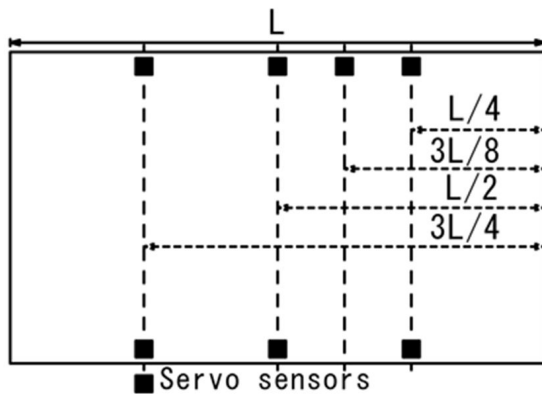


Figure 1: Example of sensor setting

3.2 ERA analysis

In the experimental modal analysis of present study, Eigensystem Realization Algorithm (ERA) [5] was applied to vibrations induced by passing vehicles. ERA needs free vibrations that were extracted from

vibration records obtained in the measurement. In Figure 2, an example of extraction of free vibration is shown. Bridge vibration was induced while a vehicle ran over the bridge. After the vehicle passed the bridge, the bridge vibration continued for a while, which was regarded as free vibration in this study. The video recording was used to confirm there was no other vehicle on the bridge during those extracted free vibrations.

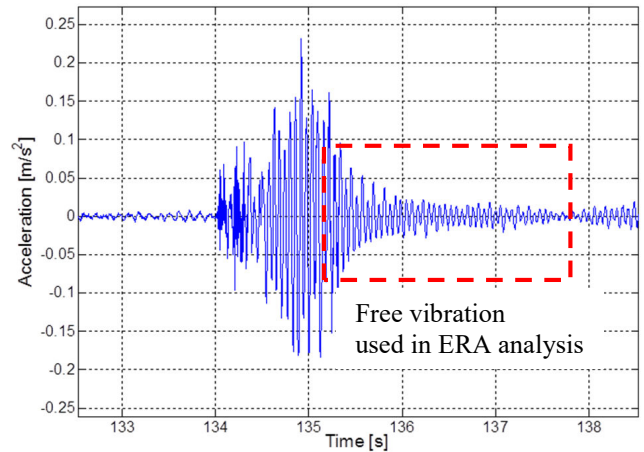


Figure 2: example of extraction of free vibration.

3.3 Screening in ERA

In ERA, physical vibration modes were identified by applying screening process based on several criteria, such as the stability of mode characteristics to the change in system order. In some cases, the damping ratio showed considerable variation with changes in system order, although the natural frequency was identified stably. In this study, the stability of the damping ratio was focused on in the identification of modal properties, as follows.

Firstly, modes corresponding to an assumed system order were identified. There were some modes that did not have a physical meaning were removed by screening in the next step. In the screening process, a stabilization diagram is used to show the stability of identified modes against system order. Figure 3 shows an example of stabilization diagram before screening which displays all the identified modes.

Unstable identified modes were then removed by screening methods. The conditions used for screening are as follows.

- Modal Assurance Criterion greater than 0.9 (1)
- Removing of negative damping (2)
- Removing damping greater than 10 % (3)
- Max Frequency difference = 0.1 (4)
- Modal amplitude ratio = 0.8~ 1.2 (5)

In Figure 4, the stabilization diagram after screening is shown. Unstable modes shown in Figure 3 were removed and stable modes only were left in Figure 4.

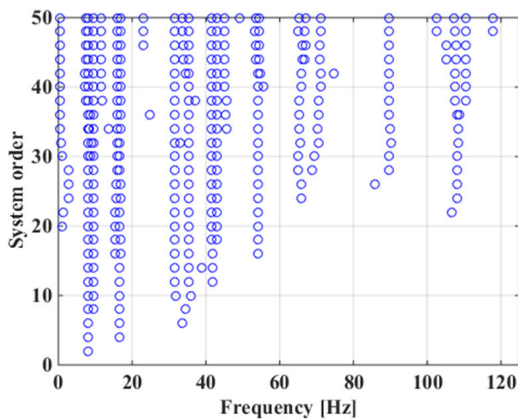


Figure 3: Stabilization diagram before screening

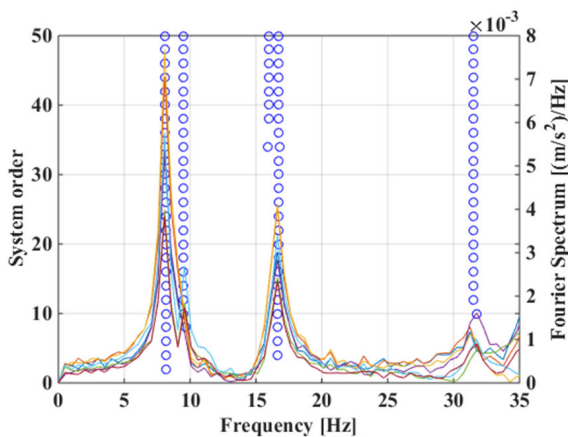


Figure 4: Stabilization diagram after screening

The stability of damping ratio was then examined. Figure 5 shows the stabilization of the damping ratio of first mode (around of 8 Hz) to the change in system order. An appropriate range of system order was then defined as follows. Firstly, the minimum system order was judged by the number of peaks in Fourier spectrum. As in Figure 4, there were three clear peaks in this example, so that the minimum system order can be judged as 6 (the number of peaks times 2). According to Figure 5, the damping ratio became stable when the system order was higher than 8. On the other hand, when system order was over 30, the damping ratio tended to vary significantly, which implied that

those system orders were too high. Thus, it was decided that the appropriate range of system order should lie between 8 and 28, in this particular case.

3.4 Identified mode shapes

Examples of mode shapes identified by ERA are shown in Figures 6 and 7. This figure shows a side view of the bridge. Circles at both ends represent support points, and others show normalized displacement at sensor positions. Sensors placed at the upstream side and those at the downstream side edge were represented by circles in different colors. As seen in Figures 6 and 7, it was difficult to understand mode shape, especially the deformation in the transverse axis of the bridge from the result of ERA. The mode shapes shown in Figures 6 and 7 are similar, although their natural frequencies are different, i.e., 8.14 Hz and 16.7 Hz. In order to understand mode shapes, theoretical modal analysis using the finite element method was conducted as described in the next section.

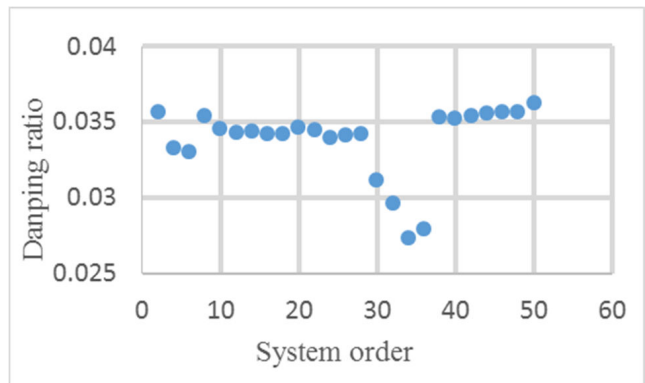


Figure 5: Stabilization of damping ratio

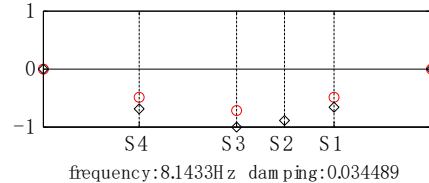


Figure 6: First mode shape identified by ERA

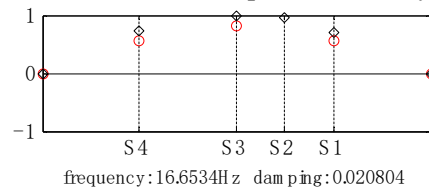


Figure 7: Third mode shape identified by ERA

4. Theoretical modal analysis

In the theoretical modal analysis, NASTRAN NX software was used. Only superstructure of the target bridges with girders and slab was modelled. As for the support conditions, spring elements were used to express rubber pads. The spring

Table 2: List of identified vibration modes

Mode No.	Mode shape name	Range of natural frequency	Mode shape of experimental analysis	Mode shape of theoretical analysis
1	Symmetric vertical bending (SV)	6.39 ~ 9.13 Hz		
2	Symmetric torsional (ST)	6.66 ~ 11.9 Hz		
3	Vertical-transverse bending (SVT)	9.76 ~ 20.8 Hz		
4	Symmetric vertical-transverse bending (AsVT)	15.9 ~ 33.9 Hz		

constant was adjusted to obtain natural frequencies close to the experimental identification.

In Table 2, the first four vibration modes identified are summarized. The first four mode shapes identified were named as symmetric vertical bending (SV, Mode 1), symmetric torsional (ST, Mode 2), symmetric vertical-transverse bending (SVT, Mode 3) and asymmetric vertical-transverse bending (AsVT, Mode 4) in this study.

5. Analytical damping evaluation

An analytical energy-based damping evaluation [6] was applied to the modal damping ratios identified. In general, the mechanism of vibration damping in a bridge is complicated and it is difficult to model accurately. However, for single-span bridges investigated in this study, the sources of damping could be limited. In this study, the damping of bridges was modeled to be provided by internal energy losses in main girders, crossbeams and rubber pads at the supports.

The damping ratio of the n th-order mode can be expressed by the ratio of the modal damping energy D_n to the modal potential energy U_n in one period (Equation 6).

$$\xi_n = \frac{D_n}{4\pi U_n} \quad (6)$$

The potential energy was assumed to be dominated by the strain energy due to the deformation corresponding to the mode shape. The damping energy was defined as the sum of the damping energy in the main girders, crossbeams and rubber

pads. The damping energy D was represented by Equation 7 that was proportional to the strain energy V of the structural components and the equivalent loss factor η .

$$D = 2\pi\eta V \quad (7)$$

The total damping energy D_n of n th-order mode was expressed as the sum of the damping energy in the main beams $D_{n,b}$, crossbeams $D_{n,c}$ and supporting part $D_{n,r}$ (Equation 8). The damping ratio of n th-order mode was obtained by Equation 8.

$$\xi_n = \frac{D_{n,b} + D_{n,c} + D_{n,r}}{4\pi U_n} \quad (8)$$

Focusing on Bridges I (new) and I (old), which had equivalent structure formats and different damping trend, the damping ratios were estimated by the energy damping evaluation method. The potential energy was calculated using the model created by the theoretical modal analysis. The loss factors were determined initially based on the results by Iino [6] and adjusted manually to obtain the damping ratios estimated close to the average values of the damping ratio identified by the ERA.

6. Results and discussion

6.1 Identified modal damping ratios

Figures 8 to 11 show the damping ratios of the four modes shown in Table 2 for all the bridges. Those four vibration modes were identified in most of the bridges. Modes 2 and 3 were observed to be relatively stable in all the bridge except Bridge 5. The identification results for Mode 2 showed

relatively large variation than those for Mode 3. It was expected initially that the identification of Mode 1 was the easiest. However, the results of the actual identification showed that there were many unidentified cases and the variation in identification was relatively large.

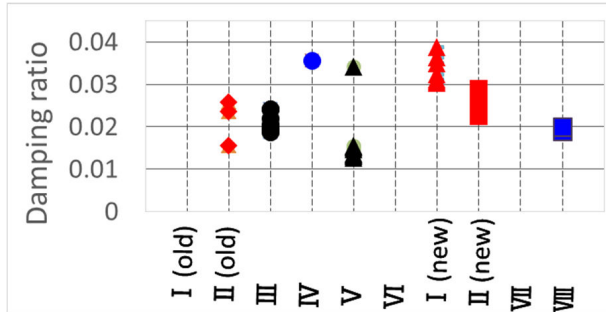


Figure 8: Damping ratio of Mode 1

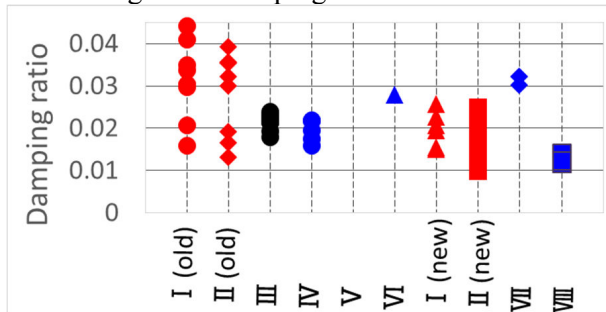


Figure 9: Damping ratio of Mode 2

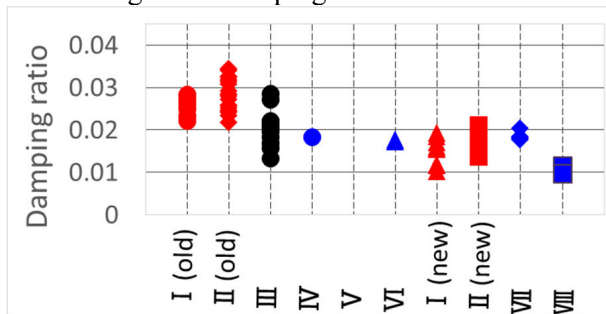


Figure 10: Damping ratio of Mode 3

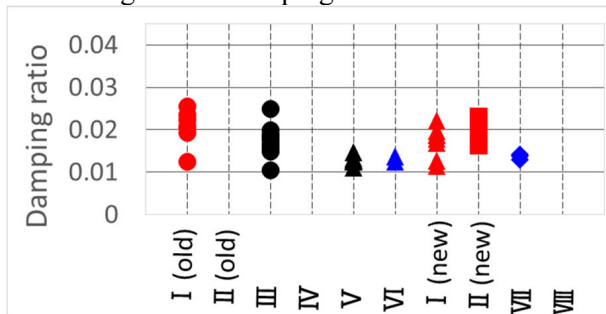


Figure 11: Damping ratio of Mode 4

6.2 Difficulty in lower order mode identification

Figures 12 and 13 show examples of stabilization diagram for the data from which the identification of lower order vibration modes was difficult. In the figures, the red arrows show the natural frequencies up to the third order mode obtained in the theory modal analysis. Those data were

obtained at Bridges I and II, which were the oldest among the measured bridges in this study. Fourier spectrum did not show clear peaks corresponding to the first two modes, as shown in Figures 12 and 13.

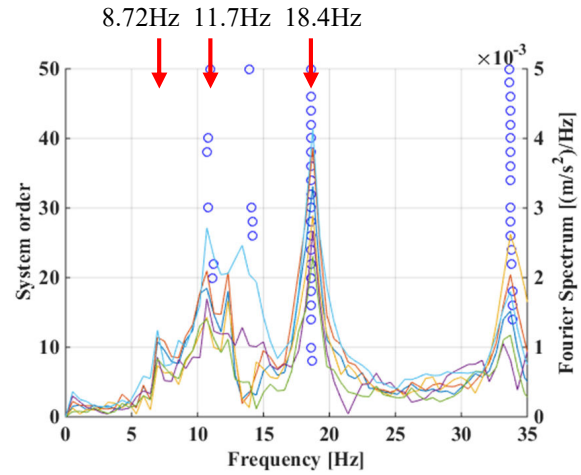


Figure 12: Stabilization diagram showing lowest order modes-Bridge I

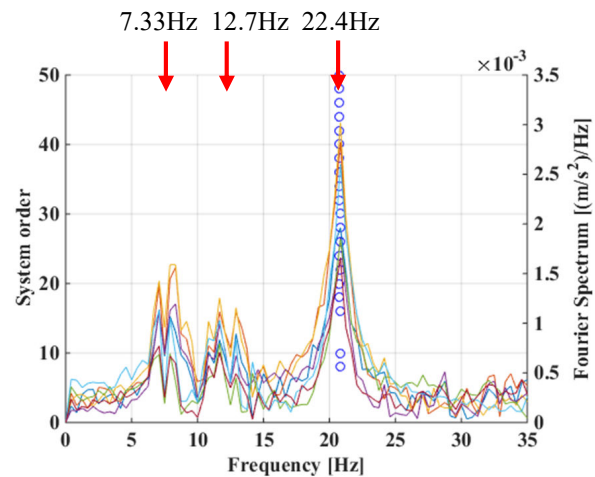


Figure 13: Stabilization diagram showing lowest order modes-Bridge II

6.3 Relationship between damping ratio and age of bridge

Here, the damping ratio of Mode 3 which showed most stable identification results is focused on. In Figure 14, the relationship between the average damping ratio of each bridges and completion year is shown. It was seen that the damping ratio of some of the old bridges were greater than the others. For those other bridges, the damping ratio of Mode 3 ranged from 0.015 to 0.02.

In Figure 15, the locations of Bridges I and II are shown. The structural format of Bridges I (new) and I (old) and Bridges II (new) and II (old) were almost identical (Table 1). The comparison of the damping ratio of Mode 3 for these pairs of bridges also show the trend that the older bridge had

greater damping than the newer bridge, as observed in Figures 16 and 17.

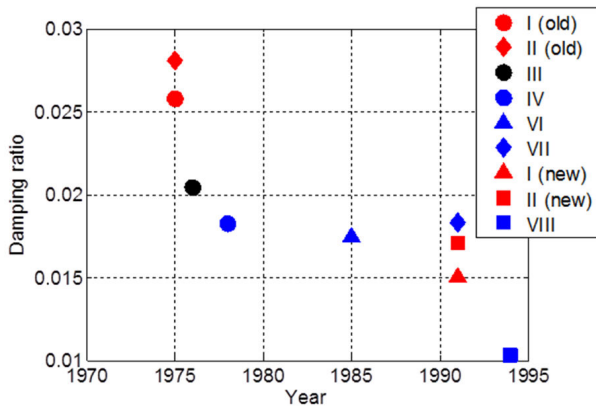


Figure 14: The average of damping ratio vs completion year

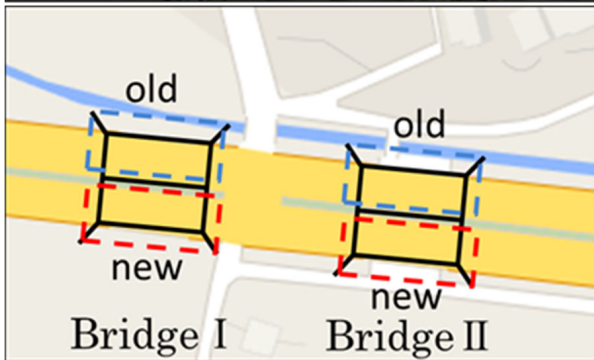


Figure 15: Location of Bridges I and II

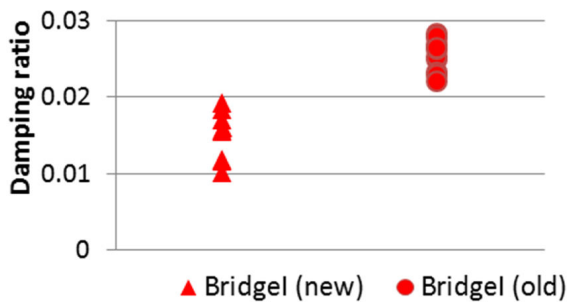


Figure 16: Comparison of damping ratio of Mode 3 for Bridge I

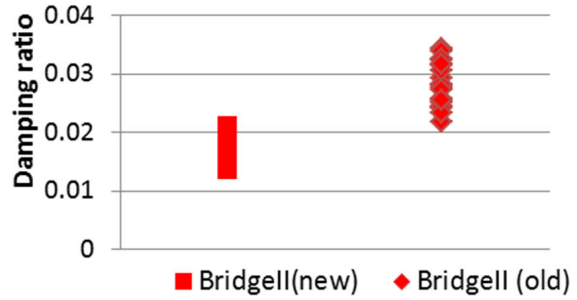


Figure 17: Comparison of damping ratio of Mode 3 for Bridge II

It was found in the previous study that damages in a concrete beam increased the damping [4]. For the selected bridges, any visible damages or deteriorations had been detected by visual inspection, and it cannot be concluded from the results in this study that the bridges with higher damping ratio might have damage or deterioration. Further study is proceeded to investigate possible reasons for the difference in damping ratio observed in the results, including the possibility that invisible damages or deteriorations resulted in different damping ratios.

6.4 Contributions of different structural components to damping

Figures 18 and 19 show the estimated contribution from different components to the damping and the average damping ratios identified by the ERA. Table 3 shows the adjusted loss factors used in the results shown in Figures 18 and 19. As observed in the figures, the contributions from different components to the damping are dependent on the vibration mode. In the lower two modes, the contributions from the main beams and supports to the damping ratios were dominant. In the higher two order modes, the contribution from the crossbeams to the damping ratios was relatively large.

For Bridge I (new) shown in Figure 18, the damping ratio identified for the SV mode was underestimated by the analytical damping evaluation as seen in the figure. Possible causes for this underestimation may include the effect of the other damping sources, such as energy dissipation to the abutment and ground. Figure 18 shows that the damping ratio of Bridge I (new) identified by the ERA decreased with increasing the mode order, with the exception of the AsVT mode. According to the contribution from each structural component shown in Figure 18, it can be understood that only crossbeams can cause an increase in the damping of fourth order mode than the third order mode.

For Bridge I (old) shown in Figure 19, the damping ratio decreased with increases in the mode order. This trend appeared to be represented reasonably by the damping model and equivalent loss factors presented in Table 3.

Figures 18 and 19 show that the damping ratios in Bridge I (old) were higher than the corresponding damping ratios in Bridge I (new). It can be seen in Table 3 that those greater damping ratios in Bridge I (old) than Bridge I (new) could be attributed to the greater equivalent loss factor for the main girders in Bridge I (old) with the loss factors for the crossbeams and supports unchanged. Although further investigation is required, the results shown above implies that, based on analytical damping evaluation, changes in a set of damping ratios can be interpreted as changes in damping in a specific structural component that could be caused by damages or deteriorations.

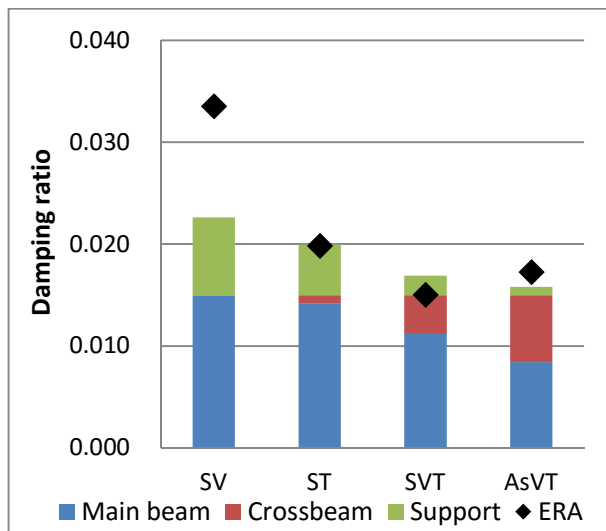


Figure 18: Damping ratio of Bridge I (new) by energy damping evaluation method

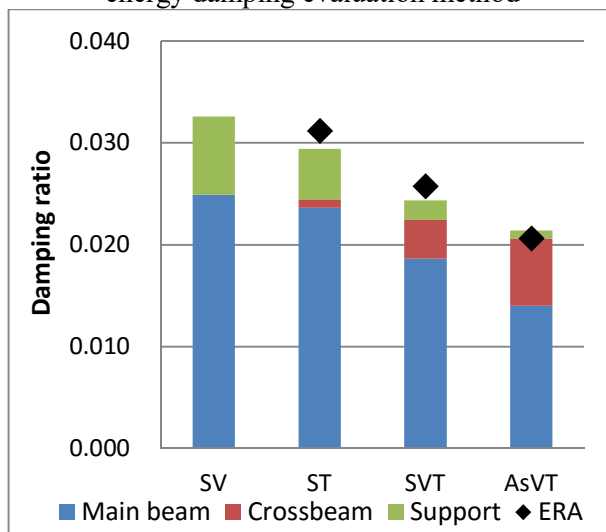


Figure 19: Damping ratio of Bridge I (old) by energy damping evaluation method

Table 3: List of loss factor

	η_b	η_c	η_r
Bridge I (new)	0.03	0.03	10
Bridge I (old)	0.05	0.03	10

7. Conclusions

The following conclusions are drawn from the results of this study.

- Four vibration modes were identified in the frequency range below about 35 Hz for the single-span PC girder bridges with a bridge length between 15 and 21 m.
- The symmetric torsional mode (Mode 2) and the vertical-transverse bending mode (Mode 3) were identified with higher stability than the other vibration modes in most bridges.
- For the third vibration mode, the damping ratios of some old bridges were greater than the damping ratios of the other bridges.
- The energy-based damping assessment described above can be used to explain the changes in damping associated with deteriorations or damages in bridges.

Reference

- [1]. Ministry of Land, Infrastructure, Transport and Tourism, "The future of standards for proper management of road structures", <http://www.mlit.go.jp/common/000986133.pdf> [Accessed 9 October 2015] (in Japanese)
- [2]. E. Matsumura, "Present aspects on inspection and diagnosis of concrete structures", Concrete Journal, Vol.39, No.6, pp.8-15, 2011. (in Japanese)
- [3]. S. Maas, A. Zurbes, D. Waldann, M. Waltering, V. Bungard, G. De Roeck, "Damage assessment of concrete structures through dynamic testing methods", Engineering Structure, Vol.34, pp.351-362, 2012.
- [4]. R.O.Curadelli, J.D.Riera, D.Ambrosini, M.G.Amani, "Damage detection by means of structural damping identification", Engineering Structure, Vol.30, pp.3497-3504, 2008.
- [5]. J. N. Juang, Applied System Identification, Prentice Hall PTR, Upper Saddle River, 1994, pp.133-147.
- [6]. A. J. Dammika, K. Kawarai, H. Yamaguchi, Y. Matsumoto, T. Yoshioka, "Analytical damping evaluation complementary to experimental structural health monitoring of bridges", J. of Bridge Engineering, ASCE, Vol.20, No.7, 04014095, 2015.

- [7]. H. Iino, “*Experimental identification of damping capacity of composite two-girder bridge and discussion based on the energy evaluation method*”, Master’s thesis, Graduate School of Science and Engineering, Saitama University, 2003. (in Japanese)